

## ■原著論文/ORIGINAL PAPER■

# Temperature Profile Behaviour during Low Temperature Oxidation of Auto-Ignition Process with Fuel Concentration Gradient

KAMARRUDIN, Nur Saifullah<sup>1,2\*</sup>, TAKAHASHI, Shuhei<sup>1</sup>, and IHARA, Tadayoshi<sup>3</sup><sup>1</sup> Graduate School of Engineering, Gifu University, 1-1 Yanagido, Gifu 501-1193, Japan<sup>2</sup> Universiti Malaysia Perlis, Pauh Putra Main Campus, Arau, Perlis 02600, Malaysia<sup>3</sup> Gifu University, 1-1 Yanagido, Gifu 501-1193, Japan

Received 23 September, 2014; Accepted 29 December, 2014

**Abstract** : An experimental study was conducted to investigate the patterns of the temperature distribution in a rapid compression machine, inside the cylinder during the auto-ignition process, with a stratified fuel distribution. In this paper, n-heptane was used as the fuel. Carbon dioxide was added in the charge mixture for measuring the temperature distribution using the infrared emission method. The fuel concentration gradient (FCG) was created by injecting the fuel from the bottom part of the cylinder followed by a time delay. The overall equivalence ratio was set to 0.6 and the compression ratio was 10. The relation between the difference of the equivalence ratios at the top and the bottom cylinder sides,  $\Delta\phi$ , and the waiting time from the injection,  $t_w$ , was investigated in advance. The data obtained showed that the low temperature oxidation process started to occur from the leaner  $\Delta\phi$  region. On the other hand, the hot flame began at the top side with a small  $\Delta\phi$  value, in contrast to the bottom side where the hot flame started with a large  $\Delta\phi$  value. The knock intensity (KI) could be weakened when a proper FCG is applied, but in the cases where the FCG is too steep or inadequate, lower combustion efficiency or a large KI would respectively occur.

**Key Words** : Temperature distribution, Emission, Carbon dioxide, Homogeneous Charge Compression Ignition, Rapid compression machine

## 1. Introduction

Homogeneous charge compression ignition (HCCI) has attracted the attention of many researchers owing to its capability to produce high efficiency like diesel engine yet lower emissions [1]. However, the heavy knock in high load conditions is one of the issues that need to be overcome [2]. In the previous research [3], we used a stratified charge by building up a fuel concentration gradient (FCG) in the combustion chamber and tried to reduce the knock intensity (KI). By applying FCG, the appearance time of the hot flame varied according to the local equivalence ratio, and KI was reduced drastically. The total ignition delay is the summation of the first induction time ( $\tau_1$ ) and the second induction time ( $\tau_2$ ). It is expected that these induction times are respectively affected by the temperature and the equivalence ratio in different ways. Therefore, it is important to distinguish the effects of the temperature and equivalence ratio on these ignition delays when the FCG is applied.

In our previous paper [4], we developed a temperature

measurement technique with an infrared emission method and conducted experiments on the auto-ignition of a lean homogeneous mixture of n-heptane and air at different equivalence ratios ( $\phi$ ) in a rapid compression machine (RCM). The results showed that the leaner mixture ( $\phi = 0.3$ ) exhibited a shorter ignition delay owing to a higher temperature at the top dead centre (TDC) compared with the richer mixture condition ( $\phi = 0.6$ ). This trend is consistent with the theoretical prediction, that is, the stoichiometric mixture elicits the shortest ignition delay at the same temperature. However, during the compression process, the leaner mixture develops a higher temperature owing to the difference in the ratio of the specific heat capacity values, and the ignition delay is affected strongly by the temperature. Our previous study also showed that a temperature distribution existed in the cylinder after the compression completion, even in the cases where the simple geometry of an RCM was used, owing to the roll-up vortex. The temperature in the roll-up vortex was normally lower than the surrounding temperature of approximately 20–40 K. Therefore, the temperature distribution may affect the ignition process as well as the FCG.

In the present paper, we measured the temperature distribution

\* Corresponding author. E-mail: saifullah@unimap.edu.my

with the stratified fuel distribution during the ignition process in RCM, using the infrared emission method. Herein, we clarify the behaviours of the cool and the hot flames in the compression ignition process, and discuss the effect of FCG and temperature distribution on KI.

## 2. Experiment Setup

An RCM has been used in this experiment to study the effect of FCG on low temperature oxidation and KI. Although the behaviour of the mixing and the combustion process in RCM is different compared with those within a reciprocating engine, an RCM has the advantage of a simplified mechanical system, and therefore a basic study can be completed with minimum uncertainties.

The schematic of the experimental apparatus is illustrated in Figure 1. The RCM used here has a bore of 65 mm and a stroke of 142 mm. The compression ratio ( $\epsilon$ ) was mainly set to be 10, and n-heptane was used as fuel. The initial pressure was 0.101 MPa, and the initial temperature was set at 298 K. The charge mixture was supplied into the combustion chamber located horizontally. The charge mixture was then compressed by the aluminum piston driven at a high pressure. The compression took approximately 30 ms, which corresponded to a rotation speed of the reciprocating engine of 1000 rpm. A pressure transducer (Kistler 6052C) was mounted on the combustor wall to monitor the pressure history in the cylinder from the beginning of the compression until approximately 30 ms after the piston reached the TDC. A small amount of CO<sub>2</sub> (4.0 %vol) was added in the charge mixture in the cylinder prior to the onset of compression for the purpose of the infrared (IR) emitter medium. A high speed infrared (HSIR) camera (Flir SC7000) was used to capture the IR emission from the CO<sub>2</sub> inside the combustion chamber, which was finally converted to temperature. In order to minimise the measurement error, radiation from CO<sub>2</sub> was filtered using a narrow band pass filter (centre wavelength of 4428 nm, width of  $\pm 57$  nm) that was placed in front of the HSIR camera. The frame rate of the HSIR camera was 3598 frames per second (fps). An optical trigger, which detects the motion of the piston, was used to synchronise the onset time of data measurement for both the pressure transducer and the HSIR camera. Since the experiments involved IR optical measurements, a sapphire glass was placed on the top of the cylinder head, and was used as the optical window.

In our previous study [5], compressions of the homogeneous and stratified charges were conducted, and noticeable differences in the pressure history profiles and KI were observed. Further investigations, especially on the temperature distribution, have been carried out in this study. For creating an FCG in the cylinder, it is important to measure and control the local

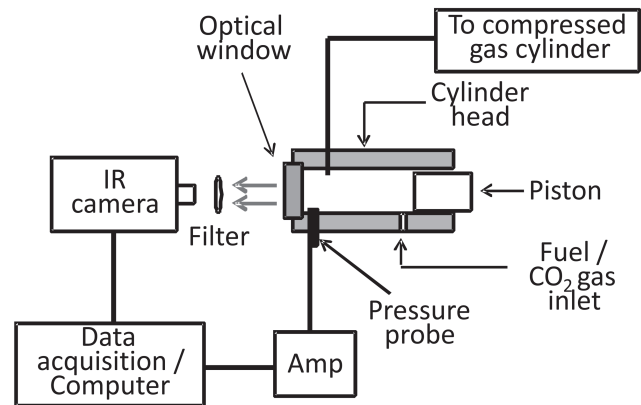


Fig.1 Schematic of experimental apparatus.

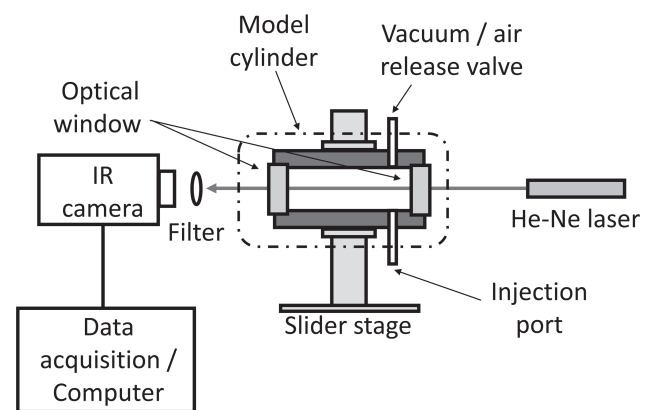


Fig.2 Experimental apparatus for measuring growth of fuel concentration gradient.

equivalence ratio ( $\phi_{local}$ ). In the experiments, we created the stratified charge by injecting the fuel in liquid form from the bottom part of the cylinder, and then let it naturally evaporate within a controlled waiting time period. Hence, we measured the relationship between the waiting time and the growth of the  $\phi_{local}$  profile using an IR laser absorption method. Figure 2 shows the experimental apparatus for the measurement of the FCG in the chamber. A model cylinder, which had the same dimension as the cylinder of the RCM, was placed on the vertical slider stage so that the height of the model cylinder could be adjusted. The positions of both the He-Ne laser ( $\lambda = 3.39 \mu\text{m}$ ) and the IR camera were fixed at the same height so that the noise to signal (N/S) ratio could be minimised. In order to calculate the local equivalence ratio at a specific elapsed time, the Lambert–Beer law was applied to estimate the absorption coefficient. The chamber was evacuated first using the vacuum pump, and the air was then introduced at 0.101 MPa. Subsequently, the fuel was injected from the injection port at the bottom of the cylinder with the syringe pump. A quartz glass was attached to the model chamber to allow laser beam access, so that the absorbed intensity could be detected by the IR camera. Five different

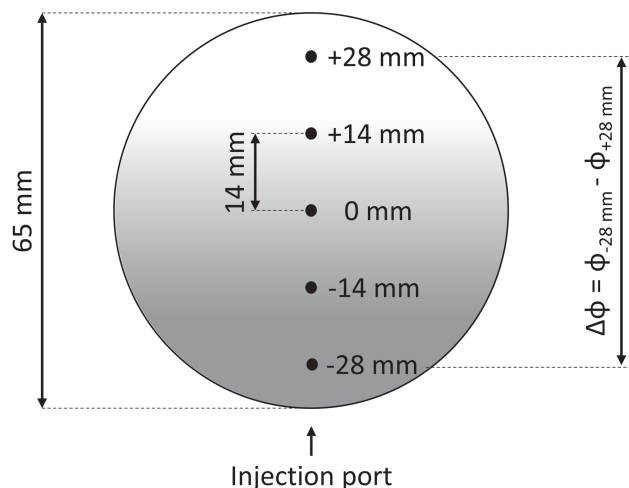


Fig.3 Definition of fuel concentration gradient.

observation point locations (at  $\pm 28$  mm,  $\pm 14$  mm, and 0 mm, from the centre of cylinder) were chosen to measure the temporal change of the local equivalence ratio, as shown in Figure 3.

The parameter  $\Delta\phi$  of the FCG was defined as the difference between the highest fuel equivalent ratio, normally recorded at the lowest point within the cylinder ( $z = -28$  mm), and the lowest equivalence ratio, which was recorded at the highest measurement point ( $z = +28$  mm), thus yielding  $\Delta\phi = \phi_{-28} - \phi_{+28}$ , as illustrated in Figure 3. For example, if the values for  $\phi_{\text{local}}$  at  $z = +28$  mm and at  $z = -28$  mm are 0.1 and 1.1, respectively, then  $\Delta\phi$  is 1.0. The elicited local equivalence ratio variation versus the waiting time ( $t_w$ ) in  $\phi_{\text{global}}$  of 0.6 is shown in Figure 4, and the corresponding  $\Delta\phi$  variation is shown in Figure 5. Note that at the lowest point in the cylinder ( $z = -28$  mm) the equivalence ratio increased at a large rate during the first 50 s, and reached a peak at approximately 60 s. As the elapsed time increased, the value of  $\phi_{\text{local}}$  at this measurement point decreased until 100 s elapsed. On the other hand, at the uppermost measurement region ( $z = 28$  mm),  $\phi_{\text{local}}$  started to increase at a moderate rate after 60 s. It subsequently increased at a slower rate until 300 s. At 300 s, all  $\phi_{\text{local}}$  values almost converged at 0.6, and at that time  $\Delta\phi$  reached the value of 0.074. On the contrary, the value of  $\Delta\phi$  peaked at approximately 60 s with a value of 1.47. With an applied FCG in the combustion chamber, the equivalence ratio is different at each point, and the specific heat capacity ratio is thus also different. Therefore, during the adiabatic compression process in the RCM, it is expected that once larger  $\Delta\phi$  values are applied a larger temperature gradient exists, that is, the higher temperature occurs at the top side of the chamber and the lower temperature on the opposite side. To create an FCG in the RCM, an air-CO<sub>2</sub> gas mixture was first introduced inside the cylinder at a pressure of 0.101 MPa. After

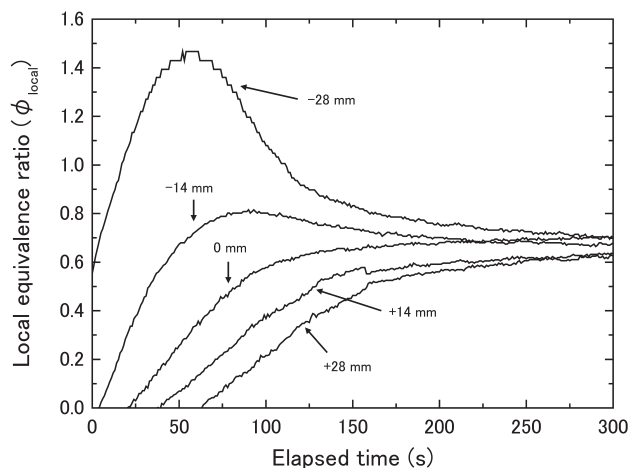


Fig.4 Growth of the equivalence ratio at various locations inside the cylinder. The pressure was 0.101 MPa and the ambient temperature was 298 K.

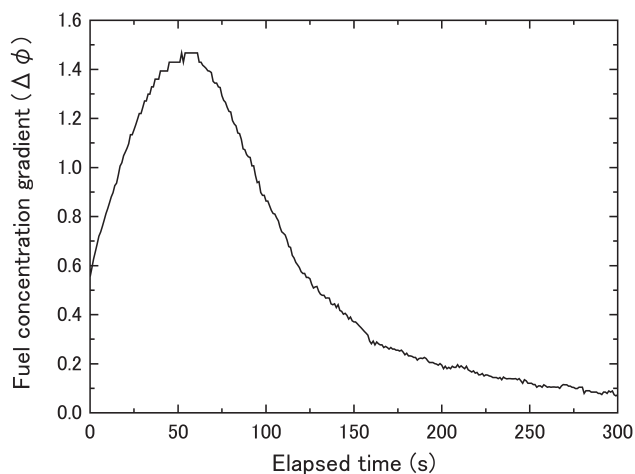


Fig.5 Change of  $\Delta\phi$  of the fuel concentration gradient (FCG) inside the cylinder. The pressure was 0.101 MPa, and the ambient temperature was 298 K.

this fuel was carefully injected from the bottom part of the cylinder it was then let to naturally evaporate for a certain elapsed time. As fuel started to evaporate upwards, the bottom part had a higher  $\phi$  compared with the upper part of the cylinder. In the present article, the total equivalence ratio was set to 0.6, at which a heavy knock was observed with a homogeneous charge, at the compression ratio value of 10. Our developed infrared emission temperature measurement system was used, which could measure the temperature distribution within the range of 650K–1000K. We conducted auto-ignition experiments at various values of  $\Delta\phi$  by changing the waiting time. We discuss below the effects of these experiments on the temperature profile and the KI.

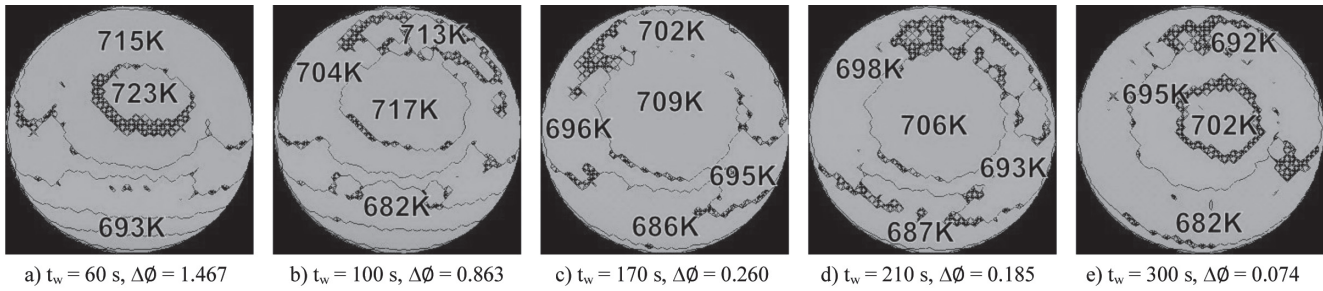


Fig.6 Temperature distributions inside the cylinder at TDC at various FCGs.

### 3. Results and Discussion

It is necessary to assess the effect of the magnitude of  $\Delta\phi$  at TDC. Figure 6 shows the temperature distribution in the cylinder at various FCGs. It was found that the temperature at the bottom part (leaner  $\phi$ ) of the cylinder was lower than that at the upper part (richer  $\phi$ ). The larger  $\Delta\phi$  is, the larger the temperature difference becomes. When the value of  $\Delta\phi$  was larger than one, the existence of horizontal layers of temperature was observed. Nevertheless, the recorded temperature at the centre part of the cylinder had the highest value in almost all cases. The reasons might be attributed to the fact that the centre part was far from the cylinder wall (which usually had a colder temperature), and to the fact that there might have been a mixing effect owing to the roll-up vortex. In Figure 6, the temperature differences were too small to recognise the FCG clearly. Hence, we focused on the temperature at the centre of the cylinder.

As shown in Figure 4, the development of the local equivalence ratio at  $z = 0$  mm,  $\phi_0$ , increased significantly within the period of 0 s to about 125 s. After that time, the growth rate of  $\phi_0$  became lower. This temporal change of  $\phi_0$  was observed as the change of temperature profiles in the centre regions shown in Figure 6, in which the temperature of the centre part decreased as a function of the waiting time from the fuel injection. Therefore, the centre temperature was 723 K at 60 s and decreased to 717 K at 100 s, whereas at subsequent times it converged to 702 K. Of course, there was some roll-up vortex mixing effect, as shown in our previous research, but we assumed that there existed a proper FCG, which was proportional to the initial FCG before compression.

Figure 7 shows the pressure history during the auto-ignition process with homogeneous and stratified mixtures, respectively. The total equivalence ratio was 0.6, and  $\Delta\phi$  was 0.074, which corresponded to the waiting time of 300 s. The recorded pressure profiles were filtered with a low pass filter (lower graph) and a high pass filter (upper graph), respectively. The cut off frequency was 5 kHz. The applied  $\Delta\phi$  value was very small, and therefore, the low pass filtered (LPF) pressure histories do not differ much, except the fact that the second induction time ( $\tau_2$ ) of the stratified

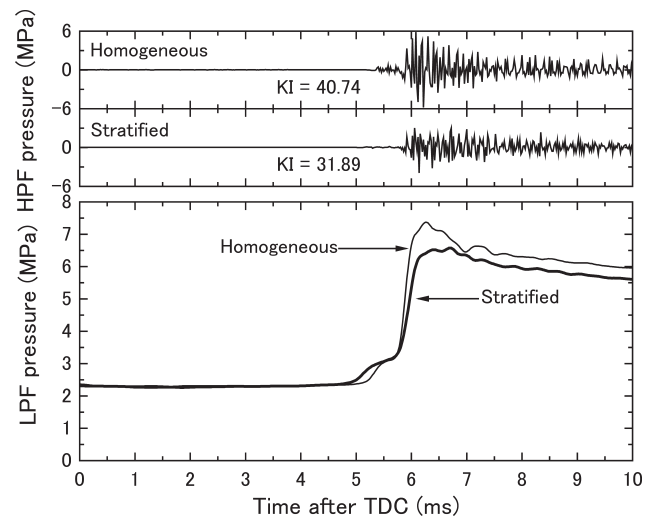


Fig.7 Pressure history during the auto-ignition process of the homogeneous and stratified charges at  $\Delta\phi = 0.074$ .

charge was a little longer. In these histories, clear two-stage ignition were observed. However, the KI was much reduced, even at small  $\Delta\phi$  values. The KI was calculated from the high pass filtered (HPF) pressure history based on the definition by Konig et al. [6],

$$KI = \frac{1}{N} \sum_{i=1}^N (p'_i - p'_{mean}) \quad (1)$$

where  $N$  is the total sampling number during knocking, and  $i$  is the sequential number of pressure datasets obtained. The sampling frequency was 50 kHz. By referring to the HPF graphs in Figure 7, the duration of the knocking was determined as the time between the start [when the value of oscillation pressure in HPF pressure differs over than 2% value of the maximum pressure ( $P_{max}$ ) in LPF graph, either in both positive or negative values], and the end (where the pressure oscillation became less than 2% of  $P_{max}$  in the LPF pressure history).

The calculated KIs were 40.74 and 31.89 for the homogeneous and the stratified charges, respectively, that is, the  $\Delta\phi$  value of 0.074 reduced the KI value to about 22%. The difference was caused owing to the temperature gradient in the stratified charge during the low temperature oxidation. Figure 8 shows the

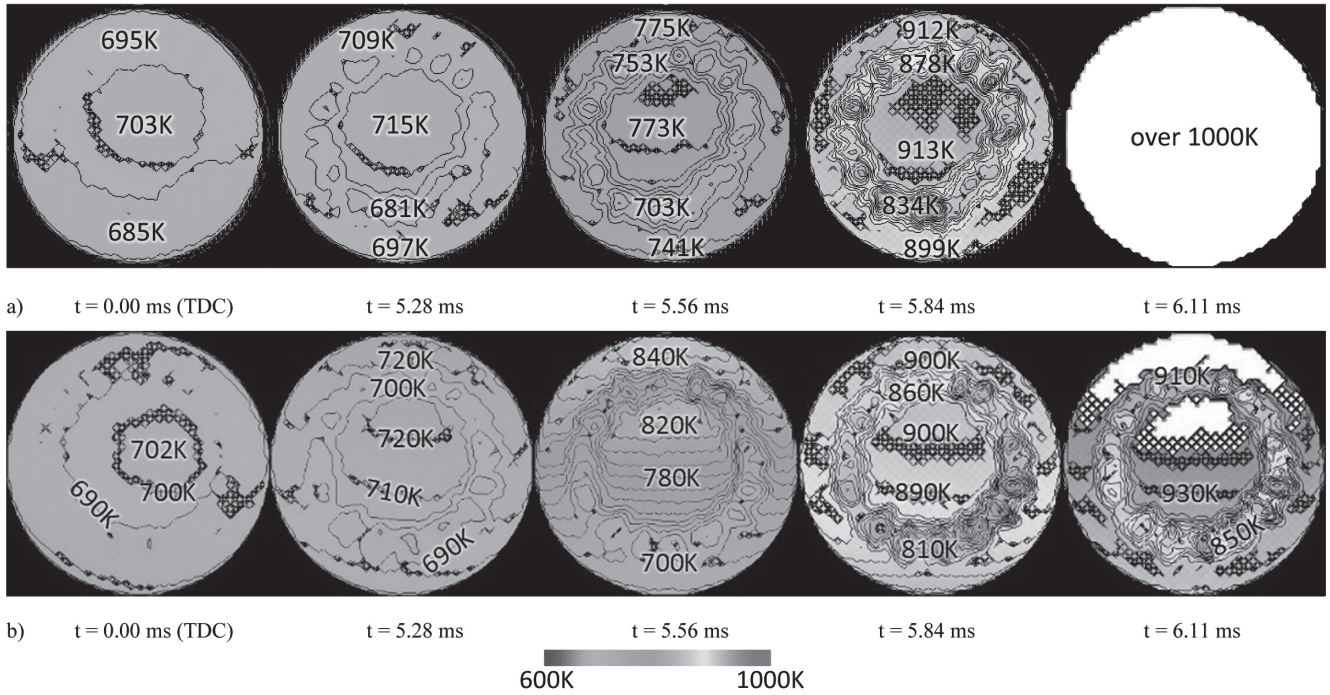


Fig.8 Temperature distributions inside the cylinder during the auto-ignition process in a) homogeneous charge, and b) stratified charge at  $\Delta\theta = 0.074$ .

temperature distribution after TDC until the appearance of the hot flame, for both studied cases. For a homogeneous charge, the temperature right after the TDC was slightly increased (within a period of 5 ms) and was almost uniform except the lower temperature ring-shape region owing to the roll-up vortex [4, 7]. The temperature increase owing to the heat release of the low temperature oxidation process was then observed. After this instance, the hot flame covered the entire cylinder. With the stratified charge, the temperature distribution after the TDC (for a period of 5.26 ms) looked similar to the homogeneous charge case. However, the obvious layered temperature distribution was observed at 5.56 ms. In the case of the above stratified charge, the equivalence ratios of the leaner  $\phi$  and the richer  $\phi$  values were estimated at 0.563 and 0.637, respectively. Therefore, the initial temperature distribution at TDC owing to the difference of the ratio of the specific heat capacity values was not so significant. However, it caused the step response in the low temperature oxidation, as shown in Figure 8b at  $t = 5.56$  ms. In addition, it was found that the layered temperature distribution was maintained at the source of the hot flame at  $t = 6.11$  ms. This large temperature difference caused the occurrence of the step response of the hot flame and reduced the magnitude of  $dP/dt$  in the LPF pressure history (which resulted in the KI reduction). It was found that the hot flame started from the leaner  $\phi$  side and moved to the richer  $\phi$  side, but the ring-shape roll-up vortex region remained as shown in Figure 8b at  $t = 6.11$  ms. This implies that the movement of the hot flame was not owing to the flame propagation, but to the succession of the auto-ignition

phenomena.

Based on the above experiment, application of the FCG in the cylinder affected the ignition delays for both the first stage and the second stage of ignition, which may provide a key to control the ignition timing in a HCCI engine. Hence, we then conducted experiments at several  $\Delta\theta$  values of the FCG in order to investigate the effect on KI. Figure 9 shows the LPF pressure profiles at varying  $\Delta\theta$ . The experimental conditions were maintained to be same as in the homogeneous compression case, i.e. for a total equivalence ratio  $\phi_{\text{global}} = 0.6$  the compression ratio  $\epsilon = 10$ , the initial pressure  $P_i = 0.101$  MPa and the initial temperature  $T_i = 298$  K. The results of Figure 9 show that the higher  $\Delta\theta$  is, the shorter the ignition delay became. This was because the low temperature oxidation process took place earlier at higher  $\Delta\theta$  values. For instance, when the  $\Delta\theta$  value was larger than 0.4, the ignition delay of the first stage became less than 3 ms. When the waiting time was 210 s or less, it was found that the pressure rise during the low temperature oxidation was gradual, whereas at larger waiting times it was stepwise. This implied that the stratified auto-ignition occurred at larger  $\Delta\theta$  conditions. On the other hand, by referring to the LPF pressure profile, the maximum pressures at large  $\Delta\theta$  values decreased and were less than 6 MPa. From the results shown in Figure 4, the local equivalence ratio at the upper part is less than 0.3 if the waiting time is less than 120 s. It is thought that the combustion efficiency drastically decreased if the mixture's equivalence ratio was less than 0.3 [8]. Therefore, when  $\Delta\theta$  was more than 0.576 ( $t_w \leq 120$  s) it was thought that the combustion efficiency was

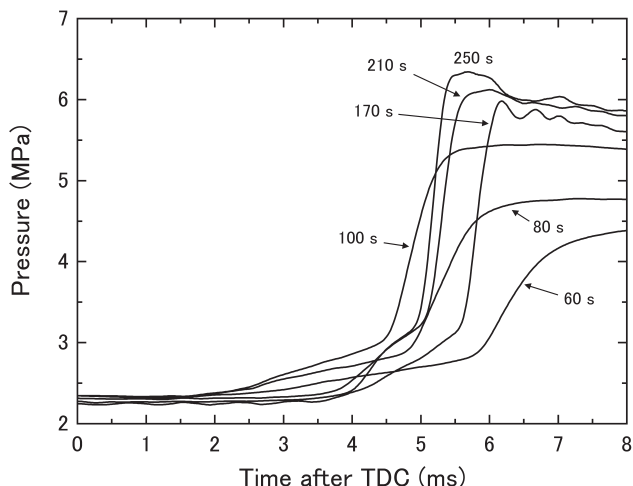


Fig.9 Pressure history during the auto-ignition process at various FCGs.  $P_i$  was 0.101 MPa,  $T_i$  was 298 K, while  $\phi_{\text{global}}$  was 0.6.

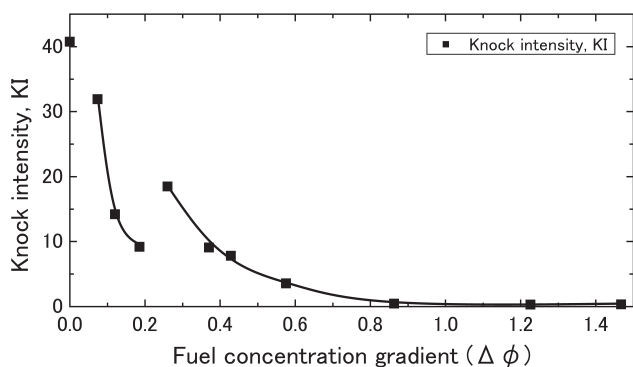


Fig.10 Knock intensity, KI, at varying  $\Delta\phi$  values calculated from the high pass filtered pressure history.

insufficient owing to the very lean mixture at the upper region of the cylinder.

Figure 10 shows the KI values at varying  $\Delta\phi$  values calculated from the HPF pressure history. From the results, the stratified charge at higher  $\Delta\phi$  values normally had lower KI values. For example, when the  $\Delta\phi$  increased from 0.074 to 1.47, KI decreased from 31.89 to 0.30 and the pressure oscillation became smaller. When the  $\Delta\phi$  was more than 0.37, the maximum pressure also decreased with increases in  $\Delta\phi$ . Therefore, it is thought that the reason for the reduction of KI is not only the effect of the locally shifted ignition, as shown in Figure 8h, but also the incomplete combustion owing to the extremely lean mixture locally. When  $\Delta\phi$  increased from 0.07 to 0.19, KI first decreased drastically. Interestingly, at FCG with  $\Delta\phi = 0.260$ , the KI value suddenly increased up to 18.4, and then started to decrease again as  $\Delta\phi$  kept increasing. A similar phenomenon was also observed in our prior research work [9], in which the value of KI in the mixture with a certain (yet a small) value of FCG was larger than its value in a homogeneous mixture. Therefore, it was found that there was an optimal  $\Delta\phi$  value for reducing KI.

Figure 11 shows the temperature distribution profiles during the auto-ignition process with  $\Delta\phi$  values of 0.12 ( $t_w = 250$  s), 0.26 ( $t_w = 170$  s), 0.37 ( $t_w = 150$  s), and 1.23 ( $t_w = 80$  s), respectively. As shown in Figure 9, the ignition delay of each condition was 4.45 ms, 3.89 ms, 3.78 ms, and 2.78 ms, respectively. The corresponding temperature distributions are shown in the second images in Figure 11a-d. Under all studied conditions, the low temperature oxidation started at the leaner  $\phi$  sides of the cylinder, where the temperature became higher owing to the larger ratio of the specific heat capacity values of the leaner mixture. When  $\Delta\phi$  was 0.12, the cool flame moved from the leaner to the richer  $\phi$  sides, and the hot flame also moved from the leaner side in a similar manner to the case of  $\Delta\phi = 0.074$ . On the other hand, when  $\Delta\phi$  was 0.37 the hot flames started from the richer  $\phi$  side of the cylinder although the cool flame started from the leaner  $\phi$  side. The difference was caused by the low local equivalence ratio of the upper side. When the waiting time was 150 s, the local equivalence ratio at the upper side was about 0.45 ( $\Delta\phi = 0.37$ ), which was near the ignition limit. In such a case, the ignition delay at the upper side became very long in spite of the high temperature owing to the lean equivalence ratio. When the waiting time was 60 s, a very large  $\Delta\phi$  value was applied to the charge. Therefore, in this case, it was expected that the local equivalence ratio in the upper region was too low to complete the combustion, and that in the lower part it was too rich, which implies that auto-ignition would also not occur. Figure 11d shows that the cool flame started at the upper part of the cylinder relative to its centre. As shown in Figure 11d, it was found that the local equivalence ratio at the leaner part was almost zero owing to the ultra-short waiting time. After the cool flame moved to the lower part, the hot flame started from the boundary of the lean and rich mixtures and moved upwards, in contrast to the case with a lower  $\Delta\phi$  value. In the case of  $\Delta\phi = 1.23$  it was obvious that the combustion efficiency was low, and this result was consistent with the low  $P_{\text{max}}$  elicited in Figure 9.

The location where the hot flame started was different in the cases of large  $\Delta\phi$  and small  $\Delta\phi$  values. When  $\Delta\phi$  was small, the hot flame started from the leaner part (as did the cool flame). On the other hand, when  $\Delta\phi$  was large, the hot flame started at the richer part (compared to the cool flame that started from the leaner side). If  $\Delta\phi$  reaches a critical value between the two cases,  $\Delta\phi_{\text{cr}}$ , it is expected that the ignition timing will be close to the same value at each local point and that it will cause a large pressure rise, thereby leading to a large KI values. Such a phenomenon can be noticed in Figure 10, where the KI at  $\Delta\phi = 0.26$  was 18.5 (and which was larger than the KI values corresponding to  $\Delta\phi = 0.12$  and  $\Delta\phi = 0.37$ ). Figure 11b, which corresponds to a value of  $\Delta\phi = 0.26$ , shows that the cool flame started from the leaner side (in the same manner as other studied



leaner  $\phi$  part and moved to the richer  $\phi$  part, since the low temperature oxidation occurred in the stratified charge successively. The pressure rise owing to the low temperature oxidation became gradual owing to the stratified ignition delay

3. After the stratified ignition of the low temperature oxidation, a relatively large temperature difference existed in the charge mixture, and the high temperature oxidation then started. The starting point of the hot flame depended on the magnitude of  $\Delta\phi$  of the FCG. When  $\Delta\phi$  was small, the hot flame moved from the top to the bottom (as did the cool flame). In contrast, when  $\Delta\phi$  was large, the hot flame moved from the bottom to the top. There was a critical  $\Delta\phi_{cr}$ , at which the total ignition delays for each of the local points became close to each other
4. The stratified occurrence of high temperature oxidation reduced the KI. With increasing  $\Delta\phi$ , KI first decreased, but then increased at  $\Delta\phi_{cr}$ . Further increases in  $\Delta\phi$  led to further KI decreases. However, excessively large  $\Delta\phi$  changes caused incomplete combustion, which resulted in a low maximum pressure

### Acknowledgments

The high speed infrared camera used was the equipment of Division of Instrumental Analysis, Life Science Research Centre of Gifu University. We are thankful to the staff for their excellent technical support.

### References

1. Yao, M., Zheng, Z., and Liu, H., *Prog. Energy Combust. Sci.* 35-5: 398-437 (2009).
2. Yelvington, P. E., and Green, W. H., *SAE paper* 2003-01-1092 (2003).
3. Qin, X., Wakai, K., Ihara, T., and Shibara, K., *J. Combust. Soc. Jpn.* (in Japanese) 48-146: 363-371 (2006).
4. Kamarrudin, N., S., Takahashi, S., Ihara, T., *J. Combust. Soc. Jpn.* (2015), in press.
5. Kamarrudin, N. S., Tanaka, S., Takahashi, S., and Ihara, T., *Proc. 9th ASPACC*, 121-124 (2013).
6. Konig, G., and Sheppard, C.G.W., *SAE Trans.* 902135: 820-839 (1990).
7. Kito, S., Wakai, K., Takahashi, S., Fukaya, N., and Takada, Y., *JSAE Review* 31-2: 373-378 (2000).
8. Furitani, M., Ohta, Y., Kono, M., and Hasegawa, M., *Proc. 4th Int. Symp. COMODIA98* (1998).
9. Ohya, T., Kamarrudin, N., S., Takahashi, S., Ihara, T., *Proc. 52nd Symp. (Japanese) Combust.* (in Japanese): 530-531 (2014).